# Intentionally Disordered Superlattices with High-DC Conductance

Enrique Diez, Angel Sánchez, and Francisco Domínguez-Adame

*Abstract*—We study disordered quantum-well-based semiconductor superlattices where the disorder is intentional and short-range correlated. Such systems consist of quantum wells of two different thicknesses randomly distributed along the growth direction, with the additional constraint that wells of one kind always appears in pairs. Imperfections due to interface roughness are considered by allowing the quantum-well thicknesses to fluctuate around their *ideal* values. As particular examples, we consider wide-gap (GaAs-Ga$_{1-x}$Al$_x$As) and narrow-gap (InAs–GaSb) superlattices. We show the existence of a band of extended states in perfect correlated disordered superlattices, giving rise to a strong enhancement of their finite-temperature dc conductance as compared to usual random ones whenever the Fermi level matches this band. This feature is seen to survive even if interface roughness is taken into account. Our predictions can be used to demonstrate experimentally that structural correlations inhibit the localization effects of disorder, even in the presence of imperfections. This effect might be the basis of new, filter-like or other specific-purpose electronic devices.

## I. Introduction

IN the past few years, a considerable amount of work has been devoted to establish that electron localization may be suppressed and bands of extended states appear in one-dimensional disordered systems whenever disorder exhibits spatial correlations [1]–[12]. This unexpected result arising from purely theoretical research is indeed important because such effect is likely to be of interest for applications. Unfortunately, these predictions have never been verified experimentally, and as a consequence there is still some controversy as to their relevance, their physical implications on transport properties, and the fabrication of new devices based on those peculiar properties. Therefore, it is crucial to find physically realizable systems to ascertain the existence of this new phenomenon. Since there has been much theoretical and experimental work in disordered semiconductor superlattices (SL's) related to localization electronic effects [13]–[15], it seems reasonable to propose random SL's with some kind of structural correlation as good candidates to check experimentally the validity of the above mentioned theoretical results. The advances achieved in molecular beam epitaxy (MBE), which allow to fabricate SL's tailored with the desired conduction- and valence-band profiles, support the feasibility of our suggestion. On the other hand, previous results of us on simple, highly idealized models of narrow-barrier SL's indicate that the effects of correlated disordered should be clearly visible in such systems [6]. Nevertheless, the theoretical description of actual SL's requires a more accurate model than the one we have previously proposed [6]. In particular, effects such as finiteness of barrier widths, nonparabolicity effects and fluctuations due to imperfections originated during growth should be taken into account. In this paper, we concern ourselves with the analysis of all those effects and study their influence on the theoretically predicted set of extended states, aiming to clarify whether those uncontrolled factors modify or not transport properties of random SL's with intentional correlated disorder.

The paper is organized as follows. In Section II, we present our system and our analytical results on transport properties (transmission coefficient and dc conductance) of intentionally disordered SL's. In the first stage, we consider the case of decoupled host bands (one-band model) and later we extend the results to narrow-gap semiconductors, using a two-band model describing nonparabolicity effects and coupling of host bands. Correlated disorder is introduced by taking quantum wells (QW's) with two different average thicknesses, placing them at random with the constraint that one of them always appears in pairs. The body of the paper is Section III, where we discuss our results on transmission coefficient and dc conductance for several temperatures. We show that the existence of bands of extended states in these structures reveals itself through well-defined peaks in the dc-conductance. In addition, we also consider imperfect SL's by allowing the QW thickness to fluctuate around their nominal values and study how this unintentional randomness affects electron transport. Results are compared with those obtained in uncorrelated disordered SL's. Finally, in Section IV, we summarize our results and give a brief explanation, at the actual experiment level, on how our predictions can be used to demonstrate experimentally that structural correlations inhibit the localization effects of disorder, concluding by suggesting possible applications of the so designed devices.

## II. Model and Theory

### A. Electronic Structure of One-Band SL's

In the simplest picture, the SL potential derives directly from the different energies of the conduction- and valence-band edges at the interfaces. A single QW consists of a layer of thickness $d_A$ of a semiconductor A embedded in

a semiconductor B. In our model of disordered SL with no imperfections, we consider that $d_A$ takes at random only two values, $a$ and $a'$. The thickness of layers B separating neighboring QW's is assumed to be the same in the whole SL, $d_B = b$. A random dimer QW SL (DQWSL) is constructed by imposing the additional constraint that QW's of thickness $a'$ appear only in pairs, called hereafter a dimer QW (DQW), as shown in Fig. 1. As already mentioned, we also discuss the case of *actual* SL's, where imperfections during growth appear. We introduce excess or defect of monolayers during growth by allowing the width of the layers of semiconductor A to fluctuate uniformly around the mean values $a$ and $a'$. Therefore, $d_A = a(1 + W\epsilon_n)$ or $d_A = a'(1 + W\epsilon_n)$, where $W$ is a positive parameter measuring the maximum deviation from the mean and $\epsilon_n$ is chosen according to a uniform probability distribution $P(\epsilon_n) = 1$ if $|\epsilon_n| < 1/2$ and zero otherwise. It is important to stress that $\{\epsilon_n\}$ is a set of random *uncorrelated* variables even when the lattice is constructed with the dimer constraint. Therefore, each QW presents a slightly different value of its thickness and resonant coupling between electronic states of neighboring wells decreases.

We focus now on electron states close to the bandgap with $k_\parallel = 0$ and use the one-band effective-mass framework to calculate the electron wave functions and allowed energies in wide-gap SL's. Within this approach, the wave function is written as a product of a band-edge orbital with a slowly varying envelope-function $F(x)$. The envelope-function satisfies a Ben Daniel–Duke equation with an effective-mass $m^*(x)$, $x$ being the coordinate along the growth direction, as follows

$$\left[ -\frac{\hbar^2}{2} \frac{d}{dx} \frac{1}{m^*(x)} \frac{d}{dx} + \sum_n V(x - x_n) \right] F(x) = E\, F(x),$$
$$(1)$$

with

$$V(x - x_n) = \begin{cases} \Delta E_c, & \text{if } |x - x_n| < b/2, \\ 0, & \text{otherwise,} \end{cases}$$

where $\Delta E_c$ is the conduction-band offset defined as $E_{cB} - E_{cA}$ and $x_n$ denotes the position of the centre of the $n$th barrier. An explicit dependence of both $E$ and $F(x)$ on quantum numbers is understood and they will be omitted in the rest of the paper. The energy is measured from the bottom of the conduction-band in the semiconductor A ($E_{cA} = 0$). Let us consider states below the barrier ($0 < E < \Delta E_c$), which are the most interesting ones to study quantum confinement effects. The corresponding envelope-function in the QW between the barriers centered at $x_n$ and $x_{n+1}$ is

$$F_n^A(x) = p_n^A e^{i\gamma(x - x_n - b/2)} + q_n^A e^{-i\gamma(x - x_n - b/2)}, \quad (2)$$

for $x_n + b/2 < x < x_{n+1} - b/2$. Here $\gamma^2 = 2m_A^* E/\hbar^2$, $m_A^*$ being the effective-mass in the QW's. $p_n^A$ and $q_n^A$ are two constants to be determined later. Inside the $n$th barrier the envelope-function can be written

$$F_n^B(x) = p_n^B e^{-\eta x} + q_n^B e^{\eta x}, \quad (3)$$

for $x_n - b/2 < x < x_n + b/2$ and now $\eta^2 = 2m_B^*(\Delta E_c - E)/\hbar^2$, $m_B^*$ being the effective-mass in the barriers. Here $p_n^B$ and $q_n^B$ are also constants.

Imposing continuity of $F(x)$ and $[m^*(x)]^{-1}dF(x)/dx$ at the interfaces, we can relate the corresponding envelope-function values at both sides of the $n$th barrier via a $2 \times 2$ transfer-matrix $M(n)$ of the form

$$\begin{pmatrix} p_n^A \\ q_n^A \end{pmatrix} = M(n) \begin{pmatrix} p_{n-1}^A \\ q_{n-1}^A \end{pmatrix} \equiv \begin{pmatrix} \alpha_n & \beta_n \\ \beta_n^* & \alpha_n^* \end{pmatrix} \begin{pmatrix} p_{n-1}^A \\ q_{n-1}^A \end{pmatrix}, \quad (4)$$

where we have defined

$$\alpha_n = \left[ \cosh(\eta b) + \frac{i}{2} \left( \frac{\gamma m_B^*}{\eta m_A^*} - \frac{\eta m_A^*}{\gamma m_B^*} \right) \sinh(\eta b) \right] e^{i\gamma(\Delta x_n - b)},$$
$$(5a)$$

$$\beta_n = -\frac{i}{2} \left( \frac{\gamma m_B^*}{\eta m_A^*} + \frac{\eta m_A^*}{\gamma m_B^*} \right) \sinh(\eta b) e^{-i\gamma(\Delta x_n - b)}, \quad (5b)$$

with $\Delta x_n \equiv x_n - x_{n-1}$, and $\alpha_n^*$ and $\beta_n^*$ are the complex conjugates of $\alpha_n$ and $\beta_n$ respectively. Letting $N$ be the total number of barriers, the transfer-matrix $T(N)$ of the SL is obtained as the product

$$T(N) = M(N)M(N-1)\cdots M(1) \equiv \begin{pmatrix} A_N & B_N \\ B_N^* & A_N^* \end{pmatrix}. \quad (6)$$

The element $A_N$ can be easily calculated recursively from the relationship [5]

$$A_n = \left( \alpha_n + \alpha_{n-1}^* \frac{\beta_n}{\beta_{n-1}} \right) A_{n-1} - \left( \frac{\beta_n}{\beta_{n-1}} \right) A_{n-2}, \quad (7)$$

supplemented by the initial conditions $A_0 = 1$, $A_1 = \alpha_1$. The knowledge of $A_N$ enables us to obtain relevant quantities like the transmission coefficient at a given energy E, $\tau(E) = 1/|A_N|^2$. Notice that these expressions are valid for any arbitrary value of QW's thicknesses and, consequently, they can be used in perfect as well as in imperfect disordered SL's within the one-band framework.

Finally, once we have computed the transmission coefficient, the dimensionless finite-temperature dc conductance can be obtained through the following expression, earlier discussed in detail by Engquist and Anderson [16]

$$\kappa(T, \mu) = \frac{\int \left( -\frac{\partial f}{\partial E} \right) \tau(E) dE}{\int \left( -\frac{\partial f}{\partial E} \right) [1 - \tau(E)]} dE, \quad (8)$$

where integrations are extended over the allowed bands, $f$ is the Fermi–Dirac distribution and $\mu$ denotes the chemical potential of the sample.

## B. Electronic Structure of Two-Band SL's

In this Section we extend our treatment to the case of disordered SL's made of narrow-gap semiconductors. Narrow-gap SL's requires a more complex analysis than those of wide-gap ones. The scalar equation arising from the effective-mass approximation is no longer valid at all. In particular, nonparabolicity effects (an energy-dependent effective-mass) must be taken into account. The simplest model that includes nonparabolicity effects and coupling of host bands is a two-band Hamiltonian obtained from the k·p theory [17], [18]. The

2

envelope-functions in the conduction- ($F_c$) and valence-band ($F_v$) satisfy the following Dirac-like equation,

$$\begin{bmatrix} E_g(x)/2 & -i\hbar v\partial \\ i\hbar v\partial & -E_g(x)/2 \end{bmatrix}\begin{bmatrix} F_c(x) \\ F_v(x) \end{bmatrix} = [E - V_g(x)]\begin{bmatrix} F_c(x) \\ F_v(x) \end{bmatrix},$$
(9)

where $\partial = d/dx$. Here $E_g(x)$ denotes the gap ($E_{gA}$ or $E_{gB}$) of each layer. $V_g(x)$ gives the absolute energy of the center of the gap and we fix the origin of energies such that it vanishes in layer $A$. The parameter $v$, having dimensions of velocity, is related to the Kane's matrix element and we will consider it as a constant in the whole superlattice. This assumption is valid in most direct gap III–V semiconductors due to the similarities of the Brillouin zone centre. Again we appeal to the transfer-matrix technique to compute the transmission coefficient. To this end, let us write down explicitly the solution of (9) as follows

$$\begin{pmatrix} F_{cn}^A(x) \\ F_{vn}^A(x) \end{pmatrix} = p_n^A\begin{pmatrix} 1 \\ \rho \end{pmatrix}e^{ik(x-x_n-b/2)} + q_n^A\begin{pmatrix} 1 \\ -\rho \end{pmatrix}e^{-ik(x-x_n-b/2)},$$
(10a)

for $x_n + b/2 < x < x_{n+1} - b/2$ and

$$\begin{pmatrix} F_{cn}^B(x) \\ F_{vn}^B(x) \end{pmatrix} = p_n^B\begin{pmatrix} 1 \\ i\lambda \end{pmatrix}e^{-qx} + q_n^B\begin{pmatrix} 1 \\ -i\lambda \end{pmatrix}e^{qx},$$
(10b)

for $x_n - b/2 < x < x_n + b/2$. For brevity, we have defined the following real parameters

$$k = \left(\frac{1}{\hbar v}\right)\sqrt{E^2 - E_{gA}^2/4},$$
(11a)

$$\rho = \frac{E - E_{gA}/2}{\hbar vk},$$
(11b)

$$q = \left(\frac{1}{\hbar v}\right)\sqrt{E_{gB}^2/4 - (E - V_B)^2},$$
(11c)

$$\lambda = \frac{E_{gB}/2 - E + V_B}{\hbar vq},$$
(11d)

where $V_B$ is the energy of the gap centre in the layer B.

Assuming the continuity of the envelope-functions at the interfaces, we obtain a $2 \times 2$ transfer-matrix $M(n)$ whose elements are now given by

$$\alpha_n = \left[\cosh(qb) + \frac{i}{2}\left(\frac{\rho}{\lambda} - \frac{\lambda}{\rho}\right)\sinh(qb)\right]e^{ik(\Delta x_n - b)},$$
(12a)

$$\beta_n = -\frac{i}{2}\left(\frac{\rho}{\lambda} + \frac{\lambda}{\rho}\right)\sinh(qb)e^{-ik(\Delta x_n - b)}.$$
(12b)

By means of the relationships (7) and (8) we can calculate recursively the transmission coefficient along the SL for the two-band model and then the dc conductance.

## C. Transmission Through a Single DQW

We now consider a single DQW as shown in Fig. 1, with the $k$th barrier in between, in an otherwise perfect and periodic SL. We are going to show that there is an specific energy value for which the so built SL is perfectly transparent. To this end, we first consider the condition for energy values to
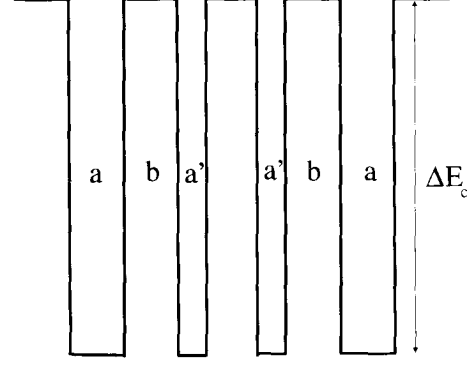


Fig. 1. Schematic diagram of the conduction-band profile of a SL containing a DQW.

be in an allowed miniband of the periodic SL, which reads in the one-band model as follows

$$\left|\cos(\gamma a)\cosh(\eta b) - \frac{1}{2}\left(\frac{\gamma m_B^*}{\eta m_A^*} - \frac{\eta m_A^*}{\gamma m_B^*}\right)\right.$$
$$\left.\cdot \sin(\gamma a)\sinh(\eta b)\right| \leq 1. \quad (13)$$

The second condition we have to take into account is simply (7) for $n = k, k + 1, k + 2$; renaming for simplicity $\alpha_k = \alpha_{k+1} \equiv \alpha'$ and $\alpha_n \equiv \alpha$ ($n \neq k, k + 1$), eliminating $A_k$ and $A_{k+1}$, and further setting $\text{Re}(\alpha') = 0$ we obtain after a little algebra

$$-A_{k+2} = (\alpha + \alpha^*)A_{k-1} - A_{k-2}.$$
(14)

Besides a constant phase factor of $\pi$, which has no effects on the magnitudes of interest, (14) reduces to (7) for a periodic SL in which barriers $k$ and $k + 1$ have been eliminated from (12) (note that for a periodic SL $\beta_n = \beta_{n-1}$). This amounts to say that the reflection coefficient at the DQW vanishes and, consequently, there exists complete transparency at the resonant energy $E_r$ satisfying $\text{Re}(\alpha') = 0$, i.e.,

$$\cos(\gamma_r a')\cosh(\eta_r b) - \frac{1}{2}\left(\frac{\gamma_r m_B^*}{\eta_r m_A^*} - \frac{\eta_r m_A^*}{\gamma_r m_B^*}\right)$$
$$\cdot \sin(\gamma_r a')\sinh(\eta_r b) = 0, \quad (15)$$

where the subscript $r$ refers to the resonant energy $E_r$. Interestingly, choosing $a'$ appropriately allows us to locate the resonant energy $E_r$ within an allowed miniband of the periodic SL, that is, the resonant energy in the range of energies given by (13). Hence, the position of the resonance for which perfect transmission exists is fixed simply from the values of the layers thickness and can be tailored as required by choosing appropriate parameters during growth.

Finally, since (7) holds also for the two-band model, a similar resonance condition can be obtained straightforwardly in narrow-gap SL's using the same arguments as before. The result is

$$\cos(k_r a)\cosh(q_r b) - \frac{1}{2}\left(\frac{\rho_r}{\lambda_r} - \frac{\lambda_r}{\rho_r}\right)\sin(k_r a)\sinh(q_r b) = 0.$$
(16)

3

Hence, since there exists also a resonance energy for which the reflection coefficient at a single DQW vanishes in the two-band framework, we can conclude that nonparabolicity effects do not suppress resonant tunneling in the DQW.

## III. TRANSPORT THROUGH A DWQSL

The above result concerning resonant tunneling through a single DQW in an otherwise periodic SL without imperfections does not imply that such a resonant phenomenon will survive in a disordered SL, that is, when more than one DQW's are randomly placed in the SL. The transfer-matrix formalism allows us to compute exactly, although not in a closed analytical fashion, the transmission coefficient and the dc conductance at finite temperature in an *arbitrary* SL. Thus, in this section we present the numerical calculation of transport magnitudes in perfect as well as in imperfect DQWSL's, aiming to elucidate whether resonant scattering is to be expected in those cases.

As a typical SL described accurately by a one-band model we have chosen a GaAs–Ga$_{0.65}$Al$_{0.35}$As structure. In this case, the conduction-band offset is $\Delta E_c = 0.25$ eV, and the effective masses are $m_A^* = 0.067$ m and $m_B^* = 0.096$ m, $m$ being the electron mass. In our computations we have taken $a = b = 32$ Å and $a' = 26$ Å. With these parameters we find from (13) only one allowed miniband below the barrier, ranging from 0.116 eV up to 0.180 eV. The resonant energy at a single DQW is $E_r = 0.141$ eV, obtained from (15), and thus it lies within the allowed miniband. To simulate imperfections, the fluctuation parameter $W$ ranges from 0 up to 0.05. The maximum value considered here represents excess or defect of several monolayers with the chosen thickness. This value is above the degree of perfection now achievable with MBE, so that the results we present are *realistic* in this sense.

As an example of a narrow-gap SL described by the two-band model we consider nearly lattice-matched InAs-GaSb SL. These two semiconductors present an almost equal Kane's matrix element leading to $\hbar v = 7.7$ eV Å, thus supporting our previous assumption that this parameter is constant through the whole SL. In our case $E_{gA} = 0.36$ eV, $E_{gB} = 0.67$ eV, and $V = 0.665$ eV, as shown in Fig. 2. We set layer thickness leading to $a = 20$ Å, $a' = 22$ Å, and $b = 40$ Å in our numerical computations. With these parameters we find, as in the one-band system, only one allowed miniband below the barrier, ranging from 0.607 eV up to 0.719 eV. From (16), we find that the resonant energy is now $E_r = 0.661$ eV.

### A. Transmission Coefficient

An example of the behavior of the transmission coefficient $\tau$ around the resonant energy $E_r$ is shown in Fig. 3 for a GaAs–Ga$_{0.65}$Al$_{0.35}$As SL with $N = 200$ barriers. In Fig. 3(a) and (b), we show results for perfect ($W = 0$) and imperfect ($W = 0.05$) DQWSL's, respectively, generated with the constraint of pairing and with a 1/2 dimer fraction. This fraction is defined as the ratio between the number of wells of width $a'$ and the total number of wells in the lattice. Since we have checked that the main conclusions of the present work are independent of this value, we take a fraction of 1/2 hereafter. As a comparison, Fig. 3(c) shows the transmission coefficient
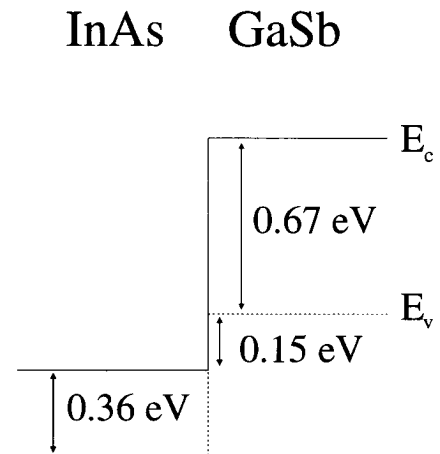
## InAs    GaSb



Fig. 2.   Schematic diagram of the conduction- and valence-band profiles in a InAs–GaSb interface.

for a perfect ($W = 0$) disordered SL without the constraint of pairing (random QWSL) with the same number of QW's of thicknesses $a$ and $a'$. We observe that for both DQWSL's close to the resonant energy $E_r$ there is an interval of energies that shows also very good transmission properties, similar to that of the resonant energy, in spite of the disordered character of the SL, even when uncorrelated fluctuations due to imperfections are present. On the contrary, this strong enhancement is not observed at all in random QWSL without pairing. We note that these results are obtained for a *specific* DQWSL; however, we have checked that for different random realizations of DQWSL's the transmission coefficient behaves similarly, with only minor changes in its fine structure.

We now discuss the details of the transmission coeffcient behavior. We can see an enlarged view of the transmission coefficient for energies very close to $E_r$ in the insets of Figs. 3(a) and 3(b). There are several narrow peaks displaying a very high value of the transmission coefficient. The number of peaks is related to the number of wells in the SL; the level spacing would only be zero in the highly ideal case of an infinite SL.[1] In Fig. 3(b), we can see also how large fluctuations destroy some of those peaks but an important number of them survive, the smaller the fluctuations the larger this number. Of course, the location of these peaks is the specific feature of particular realizations of DQWSL's. From Fig. 3(c), we conclude that in perfect random QWSL's those peaks are absent, thus indicating localization of electrons, in contrast to the situation described in DWQSL's. Therefore, the loss of quantum coherence of states close to $E_r$ is much more dramatic in perfect random QWSL's than in those DQWSL's with relatively large fluctuations, suggesting that inhibition of localization by structural correlations is, in fact, a *robust* effect.

For brevity we do not show the corresponding results for the two-band model because the qualitative features are exactly the same. Thus, resonant scattering is not destroyed by nonparabolicity effects and coupling of host bands. We do

---

[1] We have confirmed this assertion by using the Poincare-map formalism developed by us in [5], which allows us to study transmission properties of a disordered SL of finite length embedded in an infinite and periodic ($d_A = a$) SL; we do not dwell further in this matter because this work is devoted to the study of realistic superlattices which can be built and measured.
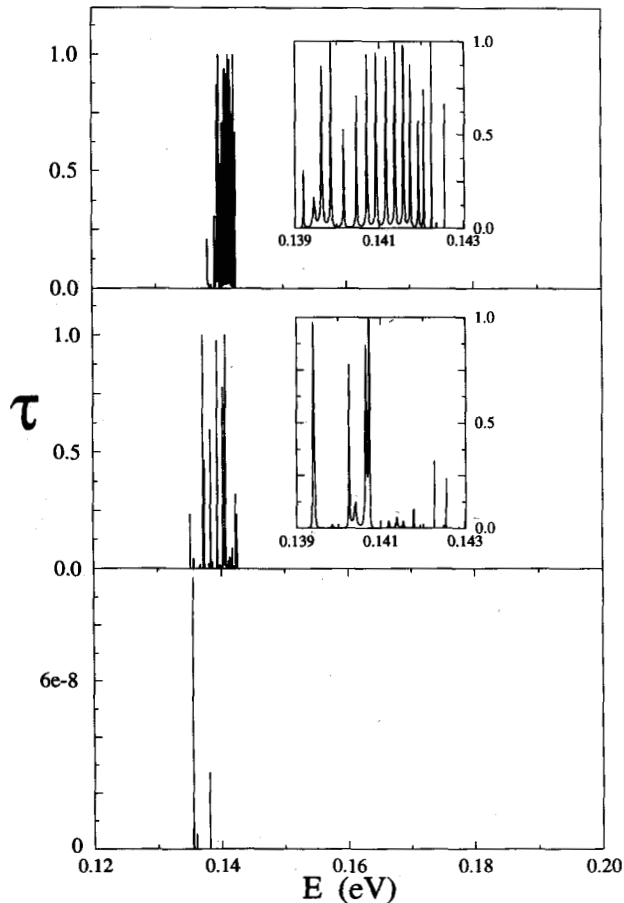
Fig. 3. Transmission coefficient $\tau$ versus energy $E$ for (a) perfect ($W = 0$) DQWSL, (b) imperfect ($W = 0.05$) DQWSL, and (c) random ($W = 0$) QWSL (c). Every GaAs–Ga$_{0.65}$Al$_{0.35}$As SL consists of $N = 200$ barriers of $b = 32$ Å whereas the thicknesses of QW are $a = 32$ Å and $a' = 26$ Å. Insets of (a) and (b) show enlarged views of the transmission coefficient around the resonant energy $E_r$. Note that the scale in (c) is much smaller than in the other two ones.
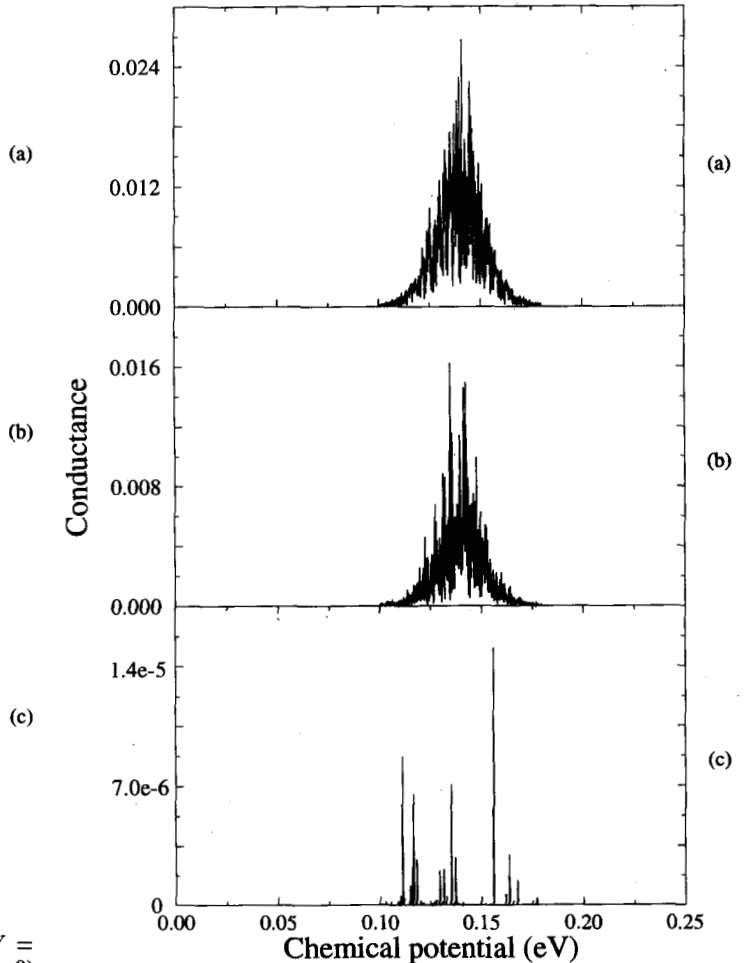


Fig. 4. dc conductance at 77 K as a function of chemical potential for (a) perfect ($W = 0$) DQWSL, (b) imperfect ($W = 0.05$) DQWSL, and (c) random ($W = 0$) QWSL. The SL's parameters are the same as in Fig. 3. Note that the scale in figure (c) is much smaller than in the other two ones.

discuss them later, in our conductance study, where we present both results for one and two-band model, so we postpone any comment to the next subsection.

### B. Finite-Temperature DC Conductance

So far, we have summarized the main properties of the DQWSL and the behavior of transmission coefficient. One of the main conclusions has been already mentioned: There is a set of extended states in the DQWSL in spite of the intentional disorder. We have provided enough theoretical evidence and then we can be quite sure of the correctness of that statement. The most important point, however, concerns applications of this result, and this immediately rises one question: Do these bands of extended states originate *experimentally* measurable features? We will answer this question in the remainder of the paper. Specifically, we will devote ourselves to show how the energy of the resonant states may be determined from finite-temperature dc conductance measurements. This would allow us to check whether the predicted energy close to $E_r$ (recall that $E_r$ depends essentially on the value of the layer thicknesses and thus it is easily determined, or else the SL can

be built as to show the desired value of $E_r$) agrees with the measured value in an experimental situation.

We have computed the electrical dc conductance by means of expression (8) for three different temperatures, 4, 77, and 300 K, and for the three kinds of SL that we are studying, namely DQWSL, DQWSL with fluctuations, and random QWSL. A global view of the results is presented in Figs. 4 and 5. In Fig. 4, the dc conductance at 77 K as a function of the chemical potential of the sample is seen for the three different SL's, with the same parameters as in Fig. 3. A marked peak of finite width in the dc conductance pattern is clearly observed whenever the chemical potential lies close to $E_r$ in the perfect DQWSL [Fig. 4(a)]. This peak persists when we add imperfections during growth, even when fluctuations are as large as a 5% [Fig. 4 (b)], and their only appreciable effect is a slight reduction of its height. On the contrary, this strong peak is not observed when DQW's are absent and the SL is purely random [Fig. 4(c)]. It is not difficult to understand why this is so. The derivative of the Fermi–Dirac function in (8) at not very high temperatures is very peaked around the chemical potential. Therefore, only when the chemical potential lies close to the set of extended states, that is to say,
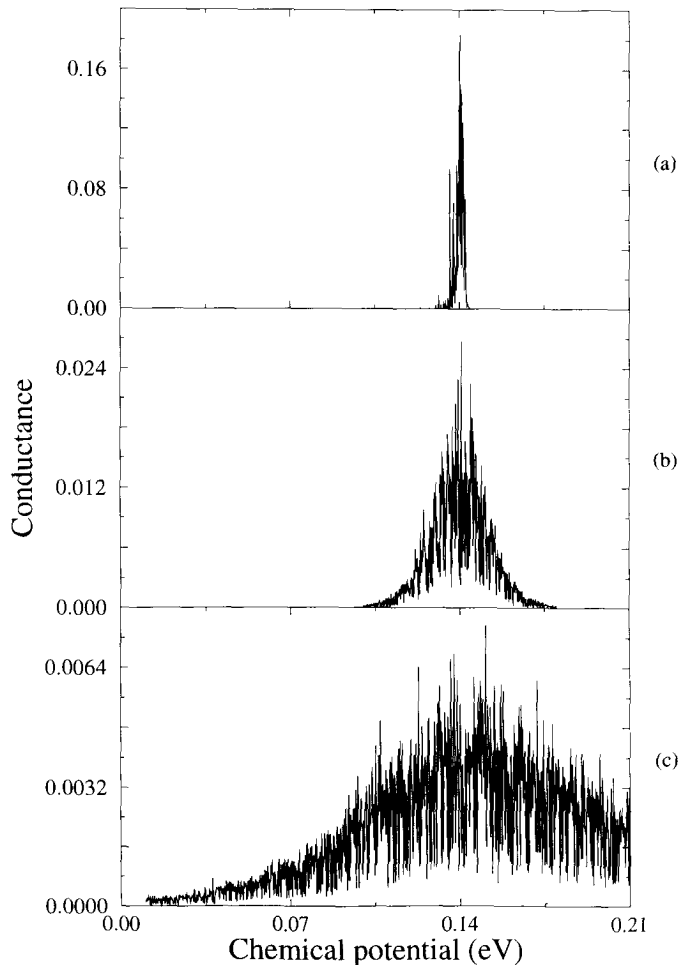
Fig. 5. dc conductance as a function of chemical potential for a DQWSL with the same parameters as in Fig. 3 at for (a) 4, (b) 77, and (c) 300 K.

Fig. 6. dc conductance at 77 K as a function of chemical potential in InAs–GaSb SL's for (a) perfect ($W = 0$) DQWSL, (b) imperfect ($W = 0.05$) DQWSL, and (c) random ($W = 0$) QWSL. Every InAs–GaSb SL consist of $N = 200$ barriers of $b = 40$ Å whereas the thicknesses of QW are $a = 20$ Å and $a' = 22$ Å. Note that the scale in (c) is much smaller than in the other two ones.

close to the resonance, there will be positive contributions to the conductance due to conducting states. Of course, if there are no extended states as in ordinary random QWSL's, never exist positive contributions and the sample will always show almost zero dc conductance.

In Fig. 5, we present the dc conductance at three different temperatures for the same DQWSL as in Fig 4. As temperature is increased, the derivative of the Fermi-Dirac function broadens and, consequently, it is not necessary to choose a chemical potential close to the resonance to obtain a high dc conductance. In fact, even if it is placed far from $E_r$ the integrals will include the contribution of the extended states, leading to an enhancement of the dc conductance. The peak height decreases because, for higher temperatures and chemical potentials very close to resonance, not only extended states are included by the Fermi-Dirac derivative in the integrals, but also a great number of localized states far from resonance, with low values of $\tau$, are weighted in the integral. The behavior we show in Figs. 4 and 5 coincides then with the intuitive expectations.

Let us now turn to narrow-gap SL's. In Fig. 6 we present the dc conductance results at 77 K obtained within the two-band framework for InAs-GaSb SL's, for perfect ($W = 0$) DQWSL, imperfect ($W = 0.05$) DQWSL and random ($W = 0$) QWSL.
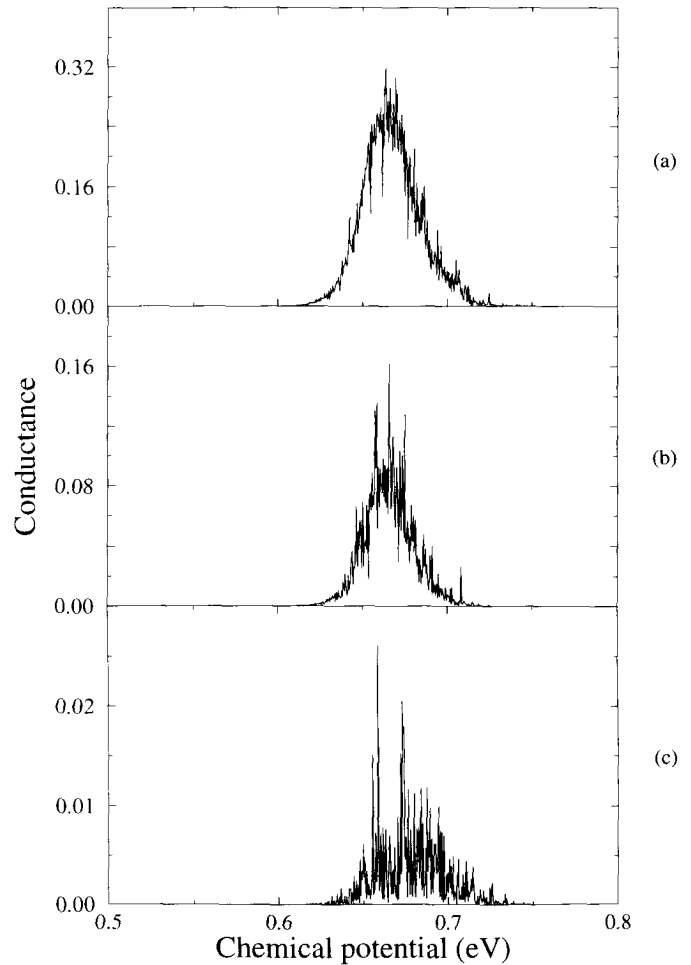
This figure shows that a strong peak of dc conductance in perfect as well as in imperfect DQWSL's is also observable in narrow-gap semiconductors, and then the discussions we present for the one-band model apply to these results as well. Once again, extended states appear when correlated disorder exists, producing a strong enhancement of dc conductance at finite temperature. This result confirms our previous statement that nonparabolicity effects and coupling of host bands do not prevent the existence of extended states.

The extended or localized nature of electronic states close to the Fermi level can be evaluated from the dependence of the dc conductance on the number of layers in the SL. The states are extended (localized) when the dc conductance is constant (decays exponentially) as the SL size increases, thus leading to an ohmic (nonohmic) behavior of the sample. In Fig. 7, we can see the dependence of the dc conductance at 77 K on the number of barriers for $\mu = E_r$ and for the three different reference systems (DQWSL without and with imperfections, and random QWSL without imperfections). In this case, we present the results of an average over 100 SL's. In the perfect DQWSL, the behavior is purely ohmic, characteristic
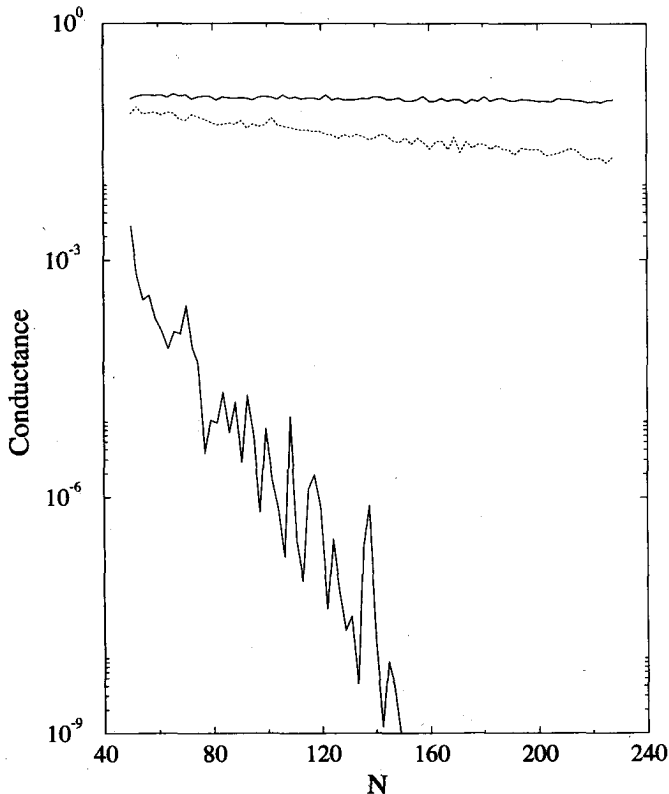
Fig. 7. dc conductance at 77 K as a function of the number of barriers in GaAs–Ga$_{0.65}$Al$_{0.35}$As for $\mu = E_r = 0.141$ eV in perfect ($W = 0$) DQWSL's (upper curve), imperfect ($W = 0.05$) DQWSL's (middle curve), and random ($W = 0$) QWSL's (lower curve). Parameters are the same as in Fig. 3. In this particular plot, we present results of averages over 100 different SL's for each case.

of extended states. When fluctuations are included, a small departure from the perfect ohmic behavior is observed, giving rise to an exponential decrease of the dc conductance as the system size increases, according to the theory of uncorrelated disordered systems (let us stress once again that fluctuations are uncorrelated). Nonohmic behavior also appears in random QWSL's, the separation from the ohmic trend being actually dramatic. Therefore, even in the presence of fluctuations, electrical conduction is much higher in imperfect DQWSL's than in perfect random QWSL's. It is then quite clear that this difference would be even larger if fluctuations are to be taken into account in random QWSL's.

From a more theoretical point of view, it is interesting to evaluate exactly the localization length at the resonant energy. This can be done computing the dc conductance at zero temperature, being nothing but $\kappa_0 \equiv \kappa(0, E_r) = \tau(E_r)/[1 - \tau(E_r)]$ from (8). The rate of the exponential decay of this magnitude versus the number of barriers—the so called Lyapunov coefficient—is the inverse of the localization lenght in units of the SL period or, in other words, the number of QW's over which the wave function spreads. For brevity we do not show here the corresponding plots since they are similar to those shown in Fig. 7, and we simply quote the main results. In GaAs–Ga$_{0.65}$Al$_{0.35}$As DQWSL's we have observed that the dependence of $\kappa_0$ with the number of barriers $N$ is of the form $\ln \kappa_0 \propto -\gamma(W)N$ where, using a least square fit, we

have obtained that $\gamma(W) = \nu W^2$ ($\nu > 0$). On the contrary, similar fits in random QWSL's give $\gamma(W) = \nu'W^2 + \gamma_0$ ($\nu' > 0$ and $\gamma_0 > 0$). Therefore, in this case the behavior is intrinsically nonohmic even in the limit $W \to 0$. However, in DQWSL's the parameter $\gamma(W)$ vanishes quadratically for small values of fluctuations, indicating that the behavior is almost ohmic. Notice that, strictly speaking, the localization length diverges only at $W = 0$ ($\gamma$ vanishes in this limit), and only in this case electronic states are truly extended. This agrees with more elaborated multifractal analysis results [5]. However, the localization length still remains very large for low level of fluctuations, so that states are almost unscattered by disorder. Therefore, they can be regarded as extended for the SL's with actually available sizes, thus contributing to electronic transport.

## IV. CONCLUSION

To summarize, we have studied transport properties at finite temperature of intentionally disordered SL's with and without DQW's. We have demonstrated that there exists a resonant energy for which electronic states remain unscattered by a single DQW in an otherwise perfect and periodic SL, due to the resonant coupling between the two neighboring QW's forming the dimer. One of the main points we have found is that these resonance effects also arise when a finite number of DQW's are randomly placed in the SL, in spite of the inherent disorder. Moreover, this result is independent of the model adopted to describe the SL, namely one- or two-band Hamiltonians. Hence, we are led to the conclusion that nonparabolicity effects and coupling of conduction- and valence-bands do not affect or qualitatively modify this phenomenon. In addition, we have demonstrated that those unscattered states reveal themselves through a dramatic enhancement of the dc conductance at finite temperature whenever the Fermi level lies close to the resonance, this effect being more apparent at low temperatures. Our present results prove that this enhancement should be experimentally observable in actual SL's since imperfections inadvertently introduced during growth do not severely affect the observed increase of the dc conductance, at least within the available degree of accuracy in MBE techniques. This is indeed an important remark from a practical viewpoint since it means that deviations of few monolayers from the ideal values of the well thicknesses cannot destroy the quantum coherence required to observe delocalization and to have dc conductance. On the contrary, those resonance phenomena are completely absent in random SL's, even if fluctuations are neglected. It is important to stress that the study of delocalization goes beyond the mere conceptual interest and, actually, new devices may be developed based in this effect. For instance, one can choose appropriate layer thicknesses ($a$, $a'$ and $b$) in such a way that $E_r$ lies close to the Fermi level of the sample, leading to the already mentioned enhancement of the dc conductance. In this way it is possible to disregard all electronic states other than unscattered ones; this may be the basis of a design of electronic filters. It is also conceivable that systems whose conductance would change abruptly with temperature could be fabricated, as for a given chemical potential the conductance of the sample

7

would jump when the temperature is such that extended states become involved. In the same way, systems with other peculiar properties of interest can be thought of.

To conclude, let us also comment that other scattering mechanisms (phonons, impurities) should also be taken into account in future works to get insight into these new phenomena. Nevertheless, on the basis of this as well as previous works, we believe that they will not modify our conclusions, inasmuch theoretical calculations on regular SL's where those effects are neglected describe to a good approximation actually built SL's. Finally, a word is in order to draw attention to this problem from the experimental viewpoint. It is clear that there is a fundamental question pertaining to basic research involved here, namely the generality of localization phenomena in physical systems. We have already discussed this implication in more theoretically oriented works [5]. Here, we want to insist instead on the fact that experimental efforts to verify the results we present are required for a better understanding of delocalization by correlated disorder. The necessity of such understanding is clear from the perspective of technological applications of SL's. The class of devices we deal with here are but a first attempt to design microelectronic systems with unexpected transport properties, its only virtue being their simplicity. Once the way is paved to the construction of other devices with exotic properties by the comprehension of the relevance of correlations, it is not difficult to realize that specific-purpose-systems could be built by using more sophisticated correlation rules. Such advances will not be possible unless the simple problem we have been discussing is understood in actually fabricated devices.

## ACKNOWLEDGMENT

## REFERENCES

[1] J. C. Flores, "Transport in models with correlated diagonal and off-diagonal disorder," *J. Phys. Condens. Matter* 1, pp. 8471–8479, 1989.
[2] P. Phillips and H.-L. Wu, "Localization and its absence: A new metallic state for conducting polymers," *Science*, vol. 252, pp. 1805–1812, 1991.
[3] A. Bovier, "Perturbation theory for the random dimer model," *J. Phys.*, vol. A 25, pp. 1021–1029, 1992.
[4] P. K. Datta, D. Giri, and K. Kundu, "Nonscattered states in a random dimer model," *Phys. Rev.*, vol. B 47, pp. 10727–10737, 1993.
[5] _____, "Nature of states in a random dimer model: Bandwidth-scaling analysis," *Phys. Rev.*, vol. 48, pp. 16347–16356, 1993.
[6] A. Sánchez and F. Domí nguez-Adame, "Enhanced suppresion of localization in the continuous Random–Dimer model," *J. Phys.*, vol. A 27, pp. 3725–3730, 1994.
[7] A. Sánchez, E. Maciá, and F. Domínguez-Adame, "Suppresion of localization in models with correlated disorder," *Phys. Rev. B*, vol. 49, pp. 147–157, 1994; Erratum, vol. 49, p. 15428, 1994.
[8] E. Diez, A. Sánchez, and F. Domínguez-Adame, " Absence of localization and large dc conductance in random superlattices with correlated disorder," *Phys. Rev. B* vol. 50, pp. 14359–14367, 1994.
[9] F. Domínguez-Adame, A. Sánchez, and E. Diez, "Quasiballistic electron transport in random superlattices," *Phys. Rev. B*, vol. 50, pp. 17736–17739, 1994.
[10] M. Hilke, "Local correlation in one- and two-dimensional discrete systems," *J. Phys. A: Math. Gen.*, vol. 27, pp. 4773–4782, 1994.
[11] A. Sánchez, F. Domínguez-Adame, G. Berman, and F. Izrailev, "Understanding delocalization in the Continuous Random Dimer model," *Phys. Rev. B*, vol. 51, pp. 6769–6772, 1995.

[12] A. Chakrabarti, S. N. Karmakar, and R. K. Moitra, "On the role of a new type of correlated disorder in extended electronic states in the Thue–Morse lattice," *Phys. Rev. Lett.*, vol. 74, pp. 1403–1406, 1995.
[13] M. Kasu, T. Yamamoto, S. Noda, and A. Sasaki, "Photoluminescence lifetime of AlAs/GaAs disordered superlattices," *Appl. Phys. Lett.*, vol. 59, pp. 800–802, 1991.
[14] X. Chen and S. Xiong, "Optical properties of GaAs/AlAs superlattices with randomly distributed layer thicknesses," *Phys. Rev. B*, vol. 47, pp. 7146–7154, 1993.
[15] A. Wakahara, T. Hasegawa, K. Kuramoto, K. V. Vong, and A. Sasaki, "Photoluminescence properties of $Si_{1-x}Ge_xSi$ disordered superlattices," *Appl. Phys. Lett.*, vol. 64, p. 1850, 1994.
[16] H. L. Engquist and P. W. Anderson, "Definition and measurement of the electrical and thermal resistances," *Phys. Rev. B*, vol. 24, pp. 1151–1154, 1981.
[17] R. Beresford, "Exact eigenfunctions of a two-band semiconductor in a uniform electric field," *Semiconduct. Sci. Technol.*, vol. 8, pp. 1957–1965, 1993.
[18] F. Domínguez-Adame and B. Méndez, "Sawtooth superlattices in a two-band semiconductor," *Semiconduct. Sci. Technol.*, vol. 9, 1358–1362, 1994.

**Enrique Diez** was born in Luzern, Switzerland, in 1969. He received the undergraduate degree in theoretical physics from the Universidad Autónoma de Madrid, Spain, in 1993.

He joined the Experimental High Energy Physics Group from Universidad Autónoma in 1991 working on the construction of ZEUS, a detector for the HERA storage ring located at DESY (Hamburg). In 1994, he joined the Universidad Carlos III de Madrid, where he is a Teaching Assistant, currently engaged in the study of quantum transport phenomena in quasiperiodic and disordered systems as well as nonlinear dynamics in solids.
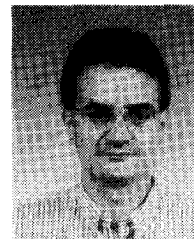
**Angel Sánchez** was born in Ourense, Galicia, Spain, in 1964. He received the undergraduate degree in physics and the Ph.D. degree in theoretical physics from the Universidad Complutense de Madrid, Spain, in 1987 and 1991, respectively.

His dissertation centered on nonlinear disordered systems of technological interest. His research activities follow that line of research, and extend to linear quasiperiodic and disordered systems. Lately, he is interested in the application of these ideas to nanostructures and on modeling of growth of semiconductor devices. In 1992, he joined the Universidad Carlos III de Madrid, where he is an Associate Professor with the Mathematics Department at the Engineering School. Since 1992, he is also a consultant with Los Alamos National Laboratory, NM.

**Francisco Domínguez-Adame** was born in 1962. He received the undergraduate degree in physics from the Universidad de Granada, Spain, in 1985 and the Ph.D. degree in semiconductor physics from the Universidad Complutense de Madrid, Spain, in 1990.

Since 1991, he is Associate Professor with the Materials Science Department at the Physics Faculty of the same University. His main research interests include optical characterization of semiconductors, electronic states in nanostructures and devices, quasiperiodic and disordered systems, and nonlinear dynamics, as well as relativistic effects in solids.